Lithuanian Journal of Physics
Vol. **66**, No. 1, pp. 20–29 (2026)
ISSN 1648-8504 eISSN 2424-3647
DOI: https://doi.org/10.3952/physics.2026.66.1.3

COULD CAROTENOIDS ADVANCE THE SENSING PROPERTIES OF KL1421 LUMINOPHORE? THEORETICAL STUDY

J. Tamulienė [a], T. Kirova [b], A. Kinens [c, d], and R. Viter [b]

[a] *Institute of Theoretical Physics and Astronomy, Vilnius University, Saulėtekio 3, 10257 Vilnius, Lithuania*
[b] *Faculty of Exact Sciences and Technologies, University of Latvia, 3 Jelgavas Street, 1004 Riga, Latvia*
[c] *Faculty of Medicine and Life Sciences, University of Latvia, 1 Jelgavas Street, 1004 Riga, Latvia*
[d] *Latvian Institute of Organic Synthesis, 21 Aizkraukles Street 21, 1006 Riga, Latvia*
Email: jelena.tamuliene@tfai.vu.lt

Received 16 May 2025; accepted 15 June 2025

This computational chemistry research was performed using Becke's three-parameter hybrid functional approach with the non-local correlation provided by Lee, Yang and Parr, and the cc-pVTZ basis set. The geometry, its change, and the charge redistribution in KL1421 when the molecule interacts with carotenoids and/or sensed molecules such as NH_3 and acetic acid were studied. The orbital diagrams were used to illustrate the excitations and their variations resulting from the formation of the above complexes. The increase in molar absorptivity is observed in compounds with carotenoids, leading to a higher absorbance of KL1421. The latter allows us to conclude that a large amount of energy could be emitted, or the emission becomes longer. Additionally, the analysis of the oscillator strengths reveals that the strong interaction among species in KL1421 could facilitate radiation emission. We concluded that carotenoids could improve the sensing properties of the KL1421 luminophore.

Keywords: luminophore, carotenoids, acetic acid, NH_3

1. Introduction

In recent decades, sensors have become valuable tools in our lives. The application of sensors is broad, ranging from measuring temperature to alarming the presence of harmful materials in the environment [1–3]. They can also be used to monitor chemical, physical and biological parameters during the bioprocess etc. The underlying principles and mechanisms of sensors are different. The electric signal is used to measure chemical properties when electrochemical sensors are used. Electromagnetic sensors capture responses to magnetic fields or electromagnetic waves. Changes in capacitance due to proximity or touch are detected by capacitive sensors. On the other hand, optical sensors sense light or changes in the optical properties. This variety of sensors has occurred due to their advantages in certain situations. For example, in a harsh environment non-contact high-precision measurements are performed mostly by optical sensors.

In many optical sensors – particularly those based on fluorescence or luminescence – the sensitivity of the luminophore is a critical component, as it directly affects the sensor's ability to detect target analytes or environmental changes. The application of luminophores in sensors requires low-cost and low-power excitation. This means that the wavelength of the excitation source should be in a range of 365–470 nm. Despite the luminophores showing a high quantum yield (over 60%), this yield depends on the excitation conditions, i.e wavelength and excitation power.

The sensitivity of optical sensors can be enhanced by increasing the light–matter interaction, which effectively increases the light fraction per unit area of the detection surface. This can be done by attaching functional nanomaterials or nanostructures to the proximity of the guiding core [4]. To improve the sensing performance of optical sensors, various strategies such as luminophore optimization, nanomaterial incorporation,

surface functionalization and signal amplification are employed. Luminophore optimization involves tailoring the photophysical and chemical properties of the dye molecule to enhance sensor performance in terms of sensitivity, stability and selectivity. Chemical modification, the incorporation of an additional molecule into a known luminophore, represents a form of luminophore optimization aimed at enhancing the overall performance of the optical sensor. So, what molecules must be incorporated to increase the effectiveness of optical sensors?

Recently, we have experimentally and theoretically investigated the properties and spectral characteristics of the KL1421 luminophore, including its interaction with water, ammonia, and acetic acid vapours [5]. A significant change in photoluminescence intensity and lifetime was observed only for the luminophore sample exposed to the acetic acid vapours [6]. These results suggest that the luminophore exhibits a selective sensing behaviour toward acetic acid vapours, as no significant photoluminescence response was observed for other tested substances.

The selective sensing of acetic acid vapours, evidenced by the lack of response to other substances, prompted a deeper investigation into improving the luminophore's detection properties. Therefore, here we pay attention to the properties of the carotenoids. These organic pigments exhibit a strong absorption in the blue–green region due to their extended conjugated systems [7–9]. The transitions to the first state of some carotenoids are forbidden due to symmetry restrictions [10, 11]. They also tend to form compounds through van der Waals interactions, hydrogen bonding, or dipole forces due to their lipophilic nature [12]. These facts are plausible to hypothesize that carotenoid incorporation into KL1421 luminophore may improve its sensing efficiency or expand its detection range.

Hence, we decided to check if the luminophore compound with carotenoids could be more sensitive, i.e. the photoluminescence response will be observed for other substances, for example, NH_3. We considered that the incorporation of carotenoids could lead to an increase in the molar absorptivity of the luminophore. This indicates the enhancement of luminophore light absorption efficiency, which can lead to the improved sensitivity of the optical sensor, provided that photoluminescence quantum yield and other photophysical properties remain favourable.

This paper presents the theoretical calculations of structure and the optical properties of novel organic luminophores with and without carotenoids/molecules NH_3 and acetic acid to evaluate the sensed properties of the KL1421 luminophore.

2. Methods of investigation

The results presented in the paper were achieved by using the Gaussian16 program [13]. The geometry of the KL1421 was obtained by B3LYP/cc-pVTZ approach [14, 15] allowing results comparable to experimental ones [16–26]. The equilibrium geometry of the compounds under study was found. The various conformers within different locations of acetic acid, NH_3, and/or selected carotenoids for the parent molecule were designed to achieve the objectives. The Onion method, along with Berny optimization, was applied to obtain the placement of the molecules in the compound and to select the lowest total energy conformer [27–29]. The optimization of the more stable conformer was repeated by applying the above ab initio approach. The frequencies were also evaluated to be sure that the position of the molecules in the compound was in an equilibrium state. The UV–Vis spectra of the compounds were calculated using the time-dependent (TD) approach [30, 31]. The molecular orbital analysis was performed to identify the transition of the electron during excitation. Butadiene and hexatriene were chosen for the study because they are the shortest carotenoids consisting of different numbers of conjugated double bonds, i.e. their ability to absorb light in the UV–visible range is different.

3. Results

The view of the molecule is depicted in Fig. 1. To exhibit the changes in the geometrical and electronic structure of the compound due to its interaction with sensing molecules, or carotenoids, we analysed the distance between N1 and N2, S and N1, the angle S–N1–C1 and the dihedral angle S–N1–C1–C2. The abovementioned distances between atoms and angles are presented in Table 1. The significant

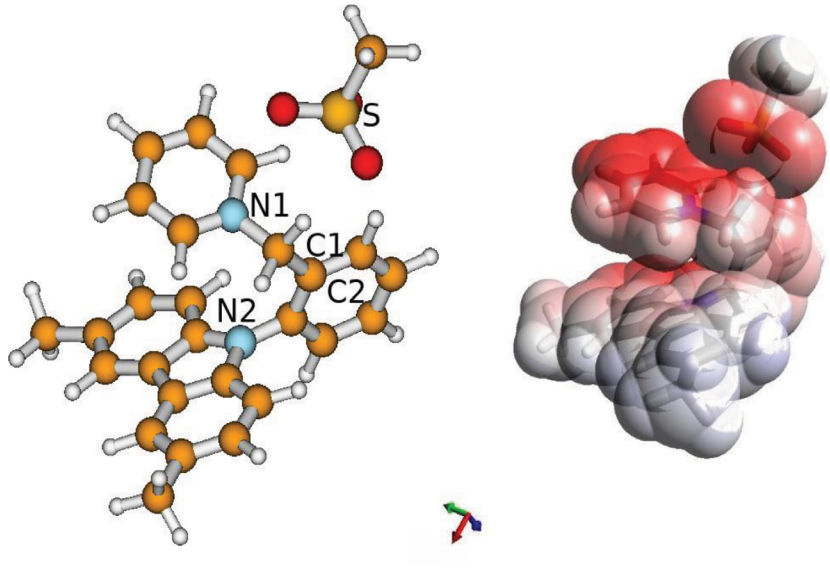

Fig. 1. The structure of the KL1421 molecule (on the left) and the Van der Waals surface (on the right) along with the electrostatic potential exhibiting the negative charge (red colour) residence. The coloured axes represent X (red), Y (green) and Z (blue) axes.

change in the distance N1–N2 should indicate the bending of the parts of the molecule or their rotation. The elongation of S–N1 or the increase of S–N1–N2 and/or S–N1–C1–C2 would indicate the changes in the position of $C_2H_3SO_4$ and, as a consequence, the significant changes in the geometrical and electronic structure due to interactions with the carotenoids and sensed species. The distances and angles were selected because the carotenoids and sensed molecules are placed near $C_2H_3SO_3$, above the rest part of the compound under study in the most stable conformers. Moreover, their placement concerning the parent molecule remains approximately the same.

Referring to the data presented in Table 1, we may state that carotenoids would slightly change the geometric structure of the KL1421 and it is independent of the conjugated double bond number (CDB): N1–N2 and S–N1 distances and S–N1–C1 and S–N1–C1–C2 angles are bigger in comparison to those of the parent molecule, but they are equal in the KL1421 compounds with butadiene and hexatriene.

The influence of the conjugated double bond number of carotenoids on the geometric structure of the parent molecule is foreseen from the analysis of the selected distances and the angles of the compounds with carotenoids together with sensed

Table 1. N1–N2 and S–N1 distances and S–N1–C1 and S–N1–C1–C2 angles exhibit the main changes in the geometrical structure of the compound under study.

Compounds	N1–N2	S–N1	S–N1–C1	S–N1–C1–C2
KL1421	3.26	3.82	72.81	–103.77
KL1421 & butadiene	3.39	3.92	77.17	–107.74
KL421 & hexatriene	3.38	3.92	77.17	–107.74
KL1421 & NH_3	3.27	3.90	73.57	–105.66
KL1421 & acetic acid	3.40	3.96	73.76	–108.45
KL1421 & butadiene & NH_3	3.38	3.95	77.65	–107.01
KL1421 & butadiene & acetic acid	3.38	3.95	77.64	–107.01
KL1421 & hexatriene & NH_3	3.45	4.03	76.09	–108.09
KL1421 & hexatriene & acetic acid	3.39	4.12	74.21	–107.26

molecules. The changes in the parameters chosen are larger in the case of hexatriene (3 CDB) than those in the case of butadiene (2 CDB) considering the influence of acetic acid and NH_3. In the case of the butadiene and sensed molecules, the geometric structure of the parent molecule is comparable to that of KL1421 & butadiene, while in the case of such kind of compounds with hexatriene, the remarkable changes of the position of $C_2H_3SO_4$ considering the parent molecule are foreseen (Table 1).

The results of the study of dipole moments indicate KL1421 as a polar molecule (Fig. 1, Table 2). So, it can form dipole–dipole interactions or hydrogen bonds. When the bond is formed with carotenoids, dipole–dipole interactions are formed due to the charge redistribution in the carotenoids which is clearly shown in Fig. 2. The non-dipole molecules become dipole due to the charge redistribution caused by KL1421. Still, the phenomenon has no significant influence on the dipole momentum of the compounds, i.e. KL1421 & butadiene or hexatriene remain with approximately the same dipole momentum as KL 1421 (Table 2).

The electronic structure of KL1421 could be changed by interaction with polar molecules such as NH_3 or acetic acid following the significant

Table 2. The dipole moment in Debye, its projection to X, Y and Z axes*, and the HOMO–LUMO gap (Gap) in eV.

Compounds	X	Y	Z	Total	Gap
KL1421	8.14	3.58	–0.52	8.91	3.14
KL1421 & butadiene	–7.98	0.12	–3.27	8.63	3.27
KL1421 & hexatriene	–7.71	2.19	–3.08	8.59	2.97
KL1421 & NH_3	6.59	3.54	–0.36	7.49	3.29
KL1421 & acetic acid	6.42	3.65	–0.87	11.16	3.36
KL1421 & butadiene & NH_3	9.54	–0.69	4.07	10.39	3.24
KL1421 & butadiene & acetic acid	9.14	–4.84	2.34	10.60	3.23
KL1421 & hexatriene & NH_3	6.91	–3.05	1.57	7.71	3.33
KL1421 & hexatriene & acetic acid	–6.84	–2.89	–0.76	7.46	3.35

* The coordinate axis orientations are different from what is possible to see in Figs. 1–2.

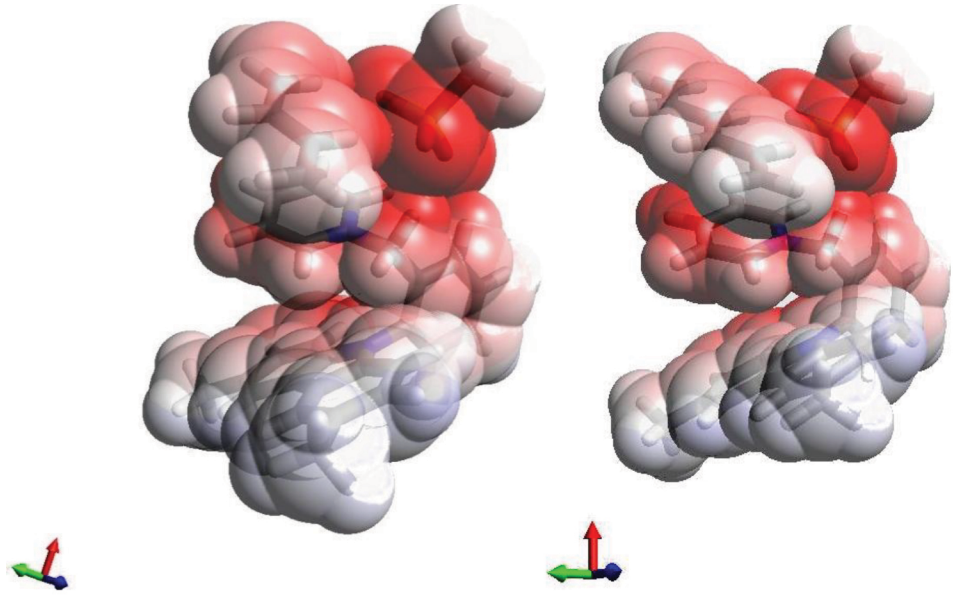

Fig. 2. The Van der Waals surface with the electrostatic potential of KL1421 & butadiene (on the left) and KL1421 & hexatriene (on the right). The coloured axes represent X (red), Y (green) and Z (blue) axes.

variations of the dipole moment of KL1421 & NH_3 or KL1421 & acetic acid (Table 2).

So, the interaction of KL1421 & butadiene with sensed molecules can increase the dipole moment of the compound (as shown in Table 2, which presents the total dipole moment of KL1421 & butadiene with NH_3 and KL1421 & butadiene with acetic acid). However, in the case of the compound containing hexatriene, this interaction decreases the total dipole moment of KL1421. Hence, the geometrical and electronic structure variations are carotenoids and sensing molecule dependent.

The interaction between KL1421 and carotenoids is strong, which follows from the analysis of the orbital diagram indicating the changes in the energy levels (Fig. 3). In the diagram, we exhibited only the energy levels involved in the sensing processes.

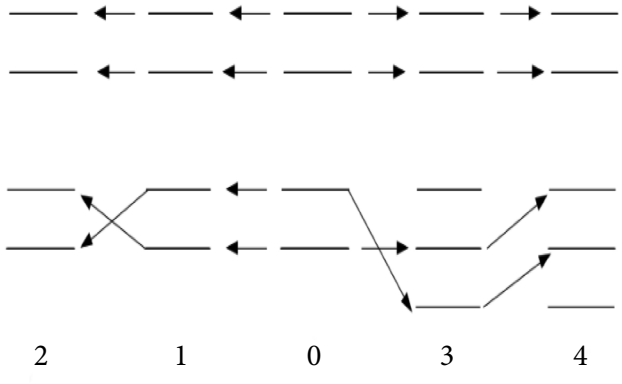

Fig. 3. The orbital diagram illustrates how the selected KL1421 orbital energy levels (number 0) are changed when the molecule approaches butadiene (3), hexatriene (4), NH_3 (1) or acetic acid (2).

The HOMO of KL1421 consists of the π type orbital of $C_2H_3SO_3$, while that in KL1421 & hexatriene is the π type orbital of this carotenoid. In KL1421 & butadiene, it is the π type orbital of $C_{14}H_{12}N$, a part of the parent molecule. The latter could be the reason for the HOMO–LUMO gap increasing in the case of the interaction of the parent molecule with butadiene, and that for decreasing in the case of hexatriene. Hence, the optical properties of KL1421 with carotenoids are conjugated double bonds number dependent. This finding also follows from the analysis of the variability of dipole moment (or the charge redistribution along with structural changes): the dipole moment of KL1421 in the presence of the carotenoids exhibits a differential decrease.

Notably, the results of the analysis of the energy level variations of KL1421 & butadiene are similar to those of KL1421 & acetic acid. In both cases, the HOMO and HOMO-1 are the π type orbital of $C_{14}H_{12}N$ and $C_2H_3SO_3$, respectively, representing similar transitions during excitation or relaxation. However, there is no orbital energy shift or splitting due to the KL1421 interaction with NH_3. So, it is rather difficult to sense this molecule with the KL1421 luminophore. This follows from the orbital diagrams illustrating a weak interaction between KL1421 and NH_3, and a strong one with acetic acid. However, these interactions become strong due to the presence of carotenoids.

Notably, the charge redistribution of the KL1421 compounds with carotenoids and that with sensed molecules is also different, as evidenced by variations in their dipole moments as well as the orbital diagram (Fig. 4). The presented orbital diagram exhibits that in the KL1421-carotenoid-sensed molecule, the charge transfer from carotenoid to KL1421 will take place. For example, in the KL1421 & butadiene & sensed molecules, HOMO is the π orbital of butadiene, so during the HOMO–LUMO excitation, the electron will be transferred from butadiene to KL1421. Table 3presents the results that demonstrate significant changes in optical properties, i.e. wavelengths and molar absorptivity changes are foreseen from the data. Moreover, the shifts are carotenoids and sensing species dependent.

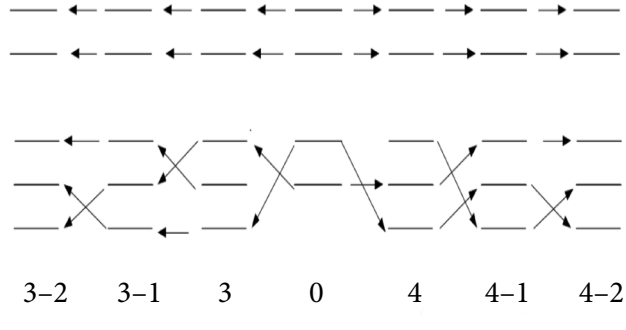

Fig. 4. The orbital diagram illustrates how the selected KL1421 orbital energy levels (number 0) are changed when the molecule approaches butadiene (3), hexatriene (4), butadiene and NH_3 (3–1), butadiene and acetic acid (3–2), hexatriene and NH_3 (4–1), or hexatriene and acetic acid (4–2).

Table 3. The wavelengths corresponding to the excitation of sensing species in the compounds KL1421 with and without carotenoids. The calculated UV–Vis spectra are not presented here because of the focus on improving the properties of KL1421 as a luminophore to be used in the sensor. Therefore, only the excitations relevant to detecting NH_3 or acetic acid are included.

Compounds	Excitation	Wavelength, nm	Molar absorptivity
KL1421 & NH_3	HOMO-3 to LUMO	339.80	40
KL1421 & acetic acid	HOMO-3 to LUMO	462.92	60
KL1421 & butadiene & NH_3	HOMO-4 to LUMO	395.91	100
KL1421 & butadiene & acetic acid	HOMO-5 to LUMO	345.65	250
KL1421 & hexatriene & NH_3	HOMO-4 to LUMO	344.24	110
KL1421 & hexatriene & acetic acid	HOMO-8 to LUMO	300.75	260

It is necessary to mention that the oscillator strengths of the excitations presented in Table 3 vary from 0.0004 to 0.0009 and from 0.0011 to 0.0028 for the KL1421 & NH_3 and KL1421 & acetic acid, respectively, with and without carotenoids. These values of oscillator strength indicate that the above transition is non-radiative. Thus, the absorbed energy would be dissipated without emitting a photon through vibrations and rotations, and the excited electron would reach the triplet state (see Fig. 5).

The excited electron transitions to the triplet state are quantum mechanically forbidden. This significantly slows the process of energy emission. As a result, the radiative transition back to the singlet state occurs at a much slower rate. Notably, in the KL1421 & carotenoids & sensed molecule, the triplet state is closer to the singlet one, but higher than the ground state in comparison to that of parent and sensed molecules (Fig. 5). This finding allows us to speculate that singlet–triplet transfer in the compounds with carotenoids will be

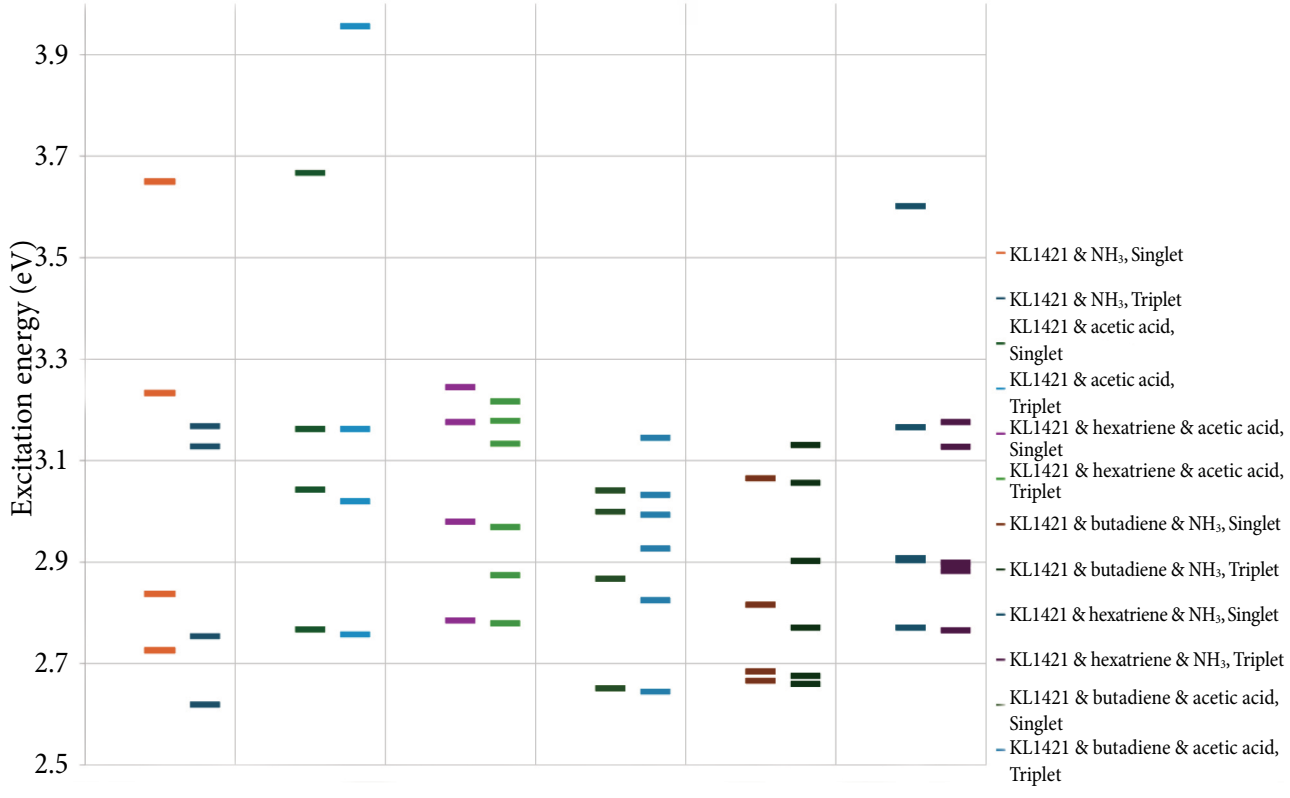

Fig. 5. The excitation energy of the singlet and triplet states concerning the ground state.

Table 4. Selected excitations correspond to the largest oscillator strength in the UV–Vis spectrum.

Compounds	Excitation	Wavelength, nm	Oscillator strength
KL1421	HOMO–LUMO	504.29	0.0044
KL1421 & butadiene	HOMO-6 to LUMO+1	336.37	0.0212
KL1421 & hexatriene	HOMO-7 to LUMO+1	320.22	0.0316
KL1421 & NH_3	HOMO to LUMO	437.09	0.0022
KL1421 & acetic acid	HOMO-3 to LUMO	358.45	0.0030
KL1421 & butadiene & NH_3	HOMO to LUMO+2	320.17	0.0307
KL1421 & butadiene & acetic acid	HOMO to LUMO+2	319.96	0.0350
KL1421 & hexatriene & NH_3	HOMO-4 to LUMO	344.24	0.0350
KL1421 & hexatriene & acetic acid	HOMO-2 to LUMO+2	281.84	0.1131

faster than that in the KL1421 & sensed molecule, while transfer from the triplet state to the ground one will be longer [32]. Notably, the inclusion of carotenoids in the KL1421 compounds does not influence the dissipation of the absorbed energy. The process of energy emission remains slow due to the transition between quantum mechanically forbidden states.

It is not surprising that the values for molar absorptivity increase remarkably due to the presence of carotenoids (Table 3). Hence, the absorbance of KL1421 becomes higher and, as a consequence, more excited energy could be emitted, or the emission becomes longer (see Table 4).

It is foreseen that in the case of KL1421 & hexatriene & acetic acid, the excitation leading to redistribution in KL1421 (no charge transfer among $C_2H_3SO_3$ and the rest part of the molecule) is allowed, i.e. radiative. So, the inclusion of carotenoids in KL1421 could improve their sensing properties not only due to its larger energy absorption or longer emission. The radiation emission of certain wavelengths could also indicate the presence of sensing species.

4. Conclusions

Referring to the results obtained, we may state that carotenoids and sensed molecules induce a slight change in the geometric structure of the parent molecule KL1421. The structural changes of KL1421 are not influenced by the conjugated double bond number of carotenoids. However, this number is important for varying the geometric structure of the parent molecule when in the KL1421 & carotenoid compound NH_3 or acetic acid is present.

The carotenoids become polar due to the charge redistribution caused by the polar KL1421. Notably, the dipole momentum of KL1421 & butadiene or hexatriene remains as it is for KL1421.

The results of our investigations exhibit that the conjugated double bond number influences the charge redistribution in the KL1421 & carotenoid & sensed molecule compounds. The interaction of KL1421 & butadiene with sensed molecules can increase the dipole moment of the compound, while that of KL1421 & hexatriene is decreased. These findings allow us to conclude that the geometrical and electronic structure variations are carotenoids and sensed molecule dependent.

The presented molecular diagrams show the strong interactions of KL1421 and carotenoids, and KL1421 & carotenoids with sensed molecules. It also exhibits the optical properties dependent on the number of the conjugated double bonds. The results of our investigation prove that NH_3 could not be sensed by KL1421, although it could be possible by KL1421 & carotenoid due to the energy level variations and the shifts of the peaks corresponding to the excitations corresponding to the charge transfer from the sensed molecule.

We also find that in the KL1421 & carotenoids & sensed molecule, the triplet state is closer to the singlet one. Hence, the singlet–triplet transfer in the compounds with carotenoids will be faster than that in the KL1421 & sensed molecule, while the transfer from the triple state to the ground one is longer and more efficient.

The molar absorptivity indicates a higher absorbance of the compound under study with carotenoids than without them. Additionally, the analysis of oscillator strength reveals that

the strong interaction among species in KL1421 & carotenoids could facilitate radiation emission.

In conclusion, the carotenoids are a good choice to improve the sensory properties of KL1421, the novel organic luminophores.

Acknowledgements

The numerical calculations with the GAUSSIAN16 package were performed using the resources of the Information Technology Research Center of Vilnius University and the Supercomputer VU HPC of Vilnius University in the Faculty of Physics.

References

[1] Z. Wu, H. Choi, and Z.M. Hudson, Achieving white-light emission using organic persistent room temperature phosphorescence, Angew. Chem. Int. Ed. **62**, e202301186 (2023), https://doi.org/10.1002/ANIE.202301186

[2] E. Amador, G. Belev, A.R. Kalapala, J. Mohapatra, Y. Wei, N. Pandey, R. Sammynaiken, J.P. Liu, W. Zhou, and W. Chen, A new pyridinium-substituted tetraphenylethylene aggregation induced emission composites for rare-earth free white light displays, Mater. Today Phys. **33**, 101036 (2023), https://doi.org/10.1016/J.MTPHYS.2023.101036

[3] K. Wu, Y. Zheng, R. Chen, Z. Zhou, S. Liu, Y. Shen, and Y. Zhang, Advances in electrochemiluminescence luminophores based on small organic molecules for biosensing, Biosens. Bioelectron. **223**, 115031 (2023), https://doi.org/10.1016/J.BIOS.2022.115031

[4] M.F.S. Ferreira, E. Castro-Camus, D.J. Ottaway, J.M. López-Higuera, X. Feng, W. Jin, Y. Jeong, N. Picqué, L. Tong, and B.M. Reinhard, Roadmap on optical sensors, J. Opt. **19**, 083001 (2017)

[5] V. Zabolotnii, J. Tamuliene, M.M. Drava, T. Kirova, I. Tepliakova, V. Lukinsone, A. Kinens, and R. Viter, Investigation of structure, optical properties and chemical stability of the KL1421 pyridinium luminophore with high quantum yield, Appl. Mater. Today **46**, 102890(2025), https://doi.org/10.1016/j.apmt.2025.102890

[6] A.B. Djurišić and Y.H. Leung, Optical properties of ZnO nanostructures, Small **2**, 944–961 (2006), https://doi.org/10.1002/SMLL.200600134

[7] M. Mimuro, U. Nagashima, S. Takaichi, Y. Nishimura, I. Yamazaki, and T. Katoh, Molecular structure and optical properties of carotenoids for the in vivo energy transfer function in the algal photosynthetic pigment system, Biochim. Biophys. Acta Bioenerg. **1098**, 271–274 (1992), https://doi.org/10.1016/S0005-2728(05)80347-0

[8] L. O'Neill, P. Lynch, M. McNamara, and H.J. Byrne, Structure property relationships in conjugated organic systems, Synth. Met. **153**, 289–292 (2005), https://doi.org/10.1016/j.synthmet.2005.07.149

[9] M.M. Mendes-Pinto, E. Sansiaume, H. Hashimoto, A.A. Pascal, A. Gall, and B. Robert, Electronic absorption and ground state structure of carotenoid molecules, J. Phys. Chem. B **117**, 11015–11021 (2013), https://doi.org/10.1021/jp309908r

[10] L. Lu, L. Shi, J. Secor, and R. Alfano, Resonance Raman scattering of β-carotene solution excited by visible laser beams into second singlet state, J. Photochem. Photobiol. B **179**, 18–22 (2018), https://doi.org/10.1016/j.jphotobiol.2017.12.022

[11] F. Qu, H. Fu, Y. Li, C. Sun, Z. Li, N. Gong, and Z. Men, Temperature effect on electronic and vibrational properties of β-carotene aggregates in aqueous ethanol solution, Dyes Pigm. **166**, 323–329 (2019), https://doi.org/10.1016/j.dyepig.2019.03.049

[12] J. Hempel, C.N. Schädle, S. Leptihn, R. Carle, and R.M. Schweiggert, Structure related aggregation behavior of carotenoids and carotenoid esters, J. Photochem. Photobiol. A Chem. **317**, 161–174 (2016), https://doi.org/10.1016/j.jphotochem.2015.10.024

[13] M.J. Frisch, G.W. Trucks, H.B. Schlegel, G.E. Scuseria, M.A. Robb, J.R. Cheeseman, G. Scalmani, V. Barone, G.A. Petersson, H. Nakatsuji, et al., *Gaussian 09 W Reference* (Gaussian, Inc., Wallingford CT, 2016) p. 139.

[14] A.D. Becke, Density functional thermochemistry. III. The role of exact exchange, J. Chem. Phys. **98**, 5648 (1993), https://doi.org/10.1063/1.464913

[15] T.H. Dunning Jr., Gaussian basis sets for use in correlated molecular calculations. I. The atoms boron through neon and hydrogen, J. Chem. Phys. **90**, 1007 (1989), https://doi.org/10.1063/1.456153

[16] R. Cardia, G. Malloci, A. Mattoni, and G. Cappellini, Effects of TIPS-functionalization and perhalogenation on the electronic, optical, and transport properties of angular and compact dibenzochrysene, J. Phys. Chem. A **118**, 5170–5177 (2014), https://doi.org/10.1021/jp502022t

[17] R. Cardia, G. Malloci, G.M. Rignanese, X. Blasé, E. Molteni, and G. Cappellini, Electronic and optical properties of hexathiapentacene in the gas and crystal phases, Phys. Rev. B **93**, 235132 (2016), https://doi.org/10.1103/PhysRevB.93.235132

[18] N. Dardenne, R. Cardia, J. Li, G. Malloci, G. Cappellini, X. Blasé, J.C. Charlier, and G.M. Rignanese, Tuning optical properties of dibenzochrysenes by functionalization: A many-body perturbation theory study, J. Phys. Chem. C **121**, 24480–24488 (2017), https://doi.org/10.1021/acs.jpcc.7b08601

[19] A. Antidormi, G. Aprile, G. Cappellini, E. Cara, R. Cardia, L. Colombo, R. Farris, M. d'Ischia, M. Mehrabanian, C. Melis, et al., Physical and chemical control of interface stability in porous Si–eumelanin hybrids, J. Phys. Chem. C **122**, 28405–28415 (2018), https://doi.org/10.1021/acs.jpcc.8b09728

[20] P. Mocci, R. Cardia, and G. Cappellini, Inclusions of Si-atoms in graphene nanostructures: A computational study on the ground-state electronic properties of coronene and ovalene, J. Phys. Conf. Ser. **956**, 012020 (2018), https://doi.org/10.1088/1742-6596/956/1/012020

[21] P. Mocci, R. Cardia, and G. Cappellini, Si-atoms substitutions effects on the electronic and optical properties of coronene and ovalene, New J. Phys. **20**, 113008 (2018), https://doi.org/10.1088/1367-2630/aae7f0

[22] A. Kumar, R. Cardia, and G. Cappellini, Electronic and optical properties of chromophores from bacterial cellulose, Cellulose **25**, 2191–2203 (2018), https://doi.org/10.1007/s10570-018-1728-0

[23] M. Szafran and J. Koput, *Ab initio* and DFT calculations of structure and vibrational spectra of pyridine and its isotopomers, J. Mol. Struct. **565**, 439–448 (2001), https://doi.org/10.1016/S0022-2860(00)00934-0

[24] D. Begue, P. Carbonniere, and C. Pouchan, Calculations of vibrational energy levels by using a hybrid ab initio and DFT quartic force field: Application to acetonitrile, J. Phys. Chem. A **109**, 4611–4616 (2005), https://doi.org/10.1021/jp0406114

[25] B. Rajakumar, P. Arathala, and B. Muthiah, Thermal decomposition of 2-methyltetrahydrofuran behind reflected shock waves over the temperature range of 1179–1361 K, J. Phys. Chem. A **125**, 5406–5422 (2021), https://doi.org/10.1021/acs.jpca.0c11490

[26] P. Arathala and R.A. Musah, Oxidation of dipropyl thiosulfinate initiated by Cl radicals in the gas phase: Implications for atmospheric chemistry, ACS Earth Space Chem. **5**, 2878–2890 (2021), https://doi.org/10.1021/acsearthspacechem.1c00246

[27] S. Dapprich, I. Komáromi, K.S. Byun, K. Morokuma, and M.J. Frisch, A new ONIOM implementation in Gaussian 98. 1. The calculation of energies, gradients and vibrational frequencies and electric field derivatives, J. Mol. Struct. (Theochem) **462**, 1–21 (1999), https://doi.org/10.1016/S0166-1280(98)00475-8

[28] T. Vreven, K.S. Byun, I. Komáromi, S. Dapprich, J.A. Montgomery Jr., K. Morokuma, and M.J. Frisch, Combining quantum mechanics methods with molecular mechanics methods in ONIOM, J. Chem. Theory Comput. **2**, 815–826 (2006), https://doi.org/10.1021/ct050289g

[29] X. Li and M.J. Frisch, Energy-represented DIIS within a hybrid geometry optimization method, J. Chem. Theory Comput. **2**, 835–839 (2006), https://doi.org/10.1021/ct050275a

[30] R. Bauernschmitt and R. Ahlrichs, Treatment of electronic excitations within the adiabatic approximation of time dependent density functional theory, Chem. Phys. Lett. **256**, 454–464 (1996), https://doi.org/10.1016/0009-2614(96)00440-X

[31] G. Scalmani, M.J. Frisch, B. Mennucci, J. Tomasi, R. Cammi, and V. Barone, Geometries and properties of excited states in the gas phase and in solution: Theory and application of a time-dependent density functional theory polarizable continuum model, J. Chem. Phys. **124**, 094107 (2006), https://doi.org/10.1063/1.2173258

[32] N. Aizawa, A. Matsumoto, and T. Yasuda, Thermal equilibration between singlet and triplet excited states in organic fluorophore for submicrosecond delayed fluorescence, Sci. Adv. **7**, eabe5769 (2021), https://doi.org/10.1126/sciadv.abe5769

AR KAROTENOIDAI GALI PAGERINTI KL1421 LIUMINOFORO JUTIKLINES SAVYBES? TEORINIS TYRIMAS

J. Tamulienė [a], T. Kirova [b], A. Kinens [c, d], R. Viter [b]

[a] *Vilniaus universiteto Teorinės fizikos ir astronomijos institutas, Vilnius, Lietuva*

[b] *Latvijos universiteto Tiksliųjų mokslų ir technologijų fakultetas, Ryga, Latvija*

[c] *Latvijos universiteto Medicinos ir gyvybės mokslų fakultetas, Ryga, Latvija*

[d] *Latvijos organinės sintezės institutas, Ryga, Latvija*

Santrauka

Pristatomų tyrimų tikslas – nustatyti, ar karotenoidai gali pagerinti KL1421 liuminoforo jutiklines savybes. Teorinis modeliavimas atliktas taikant vieną iš tankio funkcionalo artinį B3LYP kartu su cc-pVTZ baze. Buvo ištirta KL1421 molekulės geometrinė ir elektroninė struktūra bei jos pokyčiai dėl šios molekulės sąveikos su karotenoidais ir (arba) aptinkamomis molekulėmis, tokiomis kaip NH_3 ir acto rūgštis. Taip pat apskaičiuotas tiriamų darinių UV–Vis spektras.

Nustatyta, kad KL1421 geometrinė ir elektroninė struktūra nežymiai kinta dėl sąveikos su karotenoidais ir aptinkamomis molekulėmis. Konjuguotų dvigubų jungčių skaičius karotenoiduose neturi įtakos minėtiems pokyčiams KL1421 karotenoido junginiuose, tačiau tampa svarbus, kai KL1421 ir karotenoidų junginyje yra NH_3 arba acto rūgšties. Taip pat nustatyta, kad KL1421 ir butadieno sąveika su aptinkamomis molekulėmis gali padidinti junginio dipolinį momentą, o KL1421 ir heksatrieno – sumažinti. Remiantis šiais rezultatais daroma išvada, kad geometrinės ir elektroninės struktūros pokyčiai priklauso nuo karotenoidų ir aptinkamų molekulių sąveikos, ką patvirtina molekulinių orbitalių analizė. Be to, nustatyta, kad tiriamų junginių optinės savybės taip pat priklauso nuo karotenoido tipo junginyje.

Analizuojant sužadinimus nustatyta, kad KL1421 negali aptikti NH_3, nors KL1421 karotenoido junginys gali tai padaryti. Molinei absorbcijai būdinga didesnė tiriamo junginio absorbcija su karotenoidais nei be jų. Apibendrinus gautus rezultatus, daroma išvada, kad karotenoidai gali pagerinti KL1421 – naujų organinių liuminoforų – aptikimo savybes.